IAI Journals.ASM.org

SpyAD, a Moonlighting Protein of Group A *Streptococcus* Contributing to Bacterial Division and Host Cell Adhesion

Marilena Gallotta,[a] Giovanni Gancitano,[a]* Giampiero Pietrocola,[b] Marirosa Mora,[a] Alfredo Pezzicoli,[a] Giovanna Tuscano,[a] Emiliano Chiarot,[a] Vincenzo Nardi-Dei,[a] Anna Rita Taddei,[c] Simonetta Rindi,[b] Pietro Speziale,[b] Marco Soriani,[a] Guido Grandi,[a] Immaculada Margarit,[a] Giuliano Bensi[a]

Novartis Vaccines and Diagnostics Srl, Siena, Italy[a]; Department of Molecular Medicine, Institute of Biochemistry, University of Pavia, Pavia, Italy[b]; Centre for High Instruments, Electron Microscopy Section, University of Tuscia, Viterbo, Italy[c]

Group A streptococcus (GAS) is a human pathogen causing a wide repertoire of mild and severe diseases for which no vaccine is yet available. We recently reported the identification of three protein antigens that in combination conferred wide protection against GAS infection in mice. Here we focused our attention on the characterization of one of these three antigens, Spy0269, a highly conserved, surface-exposed, and immunogenic protein of unknown function. Deletion of the *spy0269* gene in a GAS M1 isolate resulted in very long bacterial chains, which is indicative of an impaired capacity of the knockout mutant to properly divide. Confocal microscopy and immunoprecipitation experiments demonstrated that the protein was mainly localized at the cell septum and could interact *in vitro* with the cell division protein FtsZ, leading us to hypothesize that Spy0269 is a member of the GAS divisome machinery. Predicted structural domains and sequence homologies with known streptococcal adhesins suggested that this antigen could also play a role in mediating GAS interaction with host cells. This hypothesis was confirmed by showing that recombinant Spy0269 could bind to mammalian epithelial cells *in vitro* and that *Lactococcus lactis* expressing Spy0269 on its cell surface could adhere to mammalian cells *in vitro* and to mice nasal mucosa *in vivo*. On the basis of these data, we believe that Spy0269 is involved both in bacterial cell division and in adhesion to host cells and we propose to rename this multifunctional moonlighting protein as SpyAD (*Streptococcus pyogenes* Adhesion and Division protein).

The Gram-positive pathogen *Streptococcus pyogenes* (group A streptococcus [GAS]) causes a broad range of human diseases, including superficial pharyngitis and skin infections, that can lead to suppurative sequelae and invasive conditions such as pneumonia, bacteremia, streptococcal toxic shock syndrome, and necrotizing fasciitis (1–4).

To exploit their infective potential, these bacteria need to survive and proliferate at the infection site and adhere to host cells, allowing colonization and/or infection of deeper tissues. Bacterial growth and host-pathogen interactions are therefore key steps toward a successful infection. To achieve this, GAS has evolved a broad repertoire of virulence factors, which exert their functions at distinct infection stages (4–7) and are regulated during different growth phases and under diverse environmental conditions (2). Among them, cell surface components mediating GAS adherence to eukaryotic cells. Different types of putative streptococcal adhesins and their cellular receptors have been identified, and extensive studies on their functional activity and expression regulation have provided important clues on their contribution to GAS tissue tropism and pathogenesis mechanisms (5–7).

A vaccine against GAS is not yet available, although several efforts have led to the discovery of putative vaccine candidates (8, 9). To attain highly selective identification of few protective GAS antigens, we recently applied a high-throughput strategy, which combines parallel mass spectrometry analysis of peptides generated after protease treatment of live bacteria, analysis of immunogenic antigens by protein array, and quantification of antibody accessible antigens by flow cytometry analysis. This allowed defining a three-protein formulation conferring consistent protection in mice against infection with multiple GAS serotypes (10, 11). Two of the three protective antigens, i.e., streptolysin O and the chemokine protease SpyCEP, were well described for their role in GAS pathogenesis (12, 13), while the function of the third antigen, Spy0269, was completely unknown and is the subject of the present study. Analysis of the publicly available GAS genomes in the NCBI database indicated that the *spy0269* gene was present in 20 out of 20 completely sequenced strains, with >93% identity along its 873-amino-acid sequence. We also reported that Spy0269 was exposed on the surface of 18 out of 22 isolates analyzed by fluorescence-activated cell sorting (FACS) using a specific mouse serum and that the protein was highly recognized by 204 out of 239 sera from pharyngitis patients, indicating high surface expression during human infection (10, 14).

Using a combination of genetic, biochemical, and cellular microbiology approaches, we provide here evidence that Spy0269, which we renamed SpyAD (*Streptococcus pyogenes* Adhesion and Division protein) is a multifunctional protein that plays a role in

Received 15 January 2014 **Returned for modification** 8 February 2014
Accepted 15 April 2014

Published ahead of print 28 April 2014

Editor: A. Camilli

Address correspondence to Immaculada Margarit, immaculada.margarit_y_ros@novartis.com, or Guido Grandi, guido.grandi@novartis.com.

* Present address: Giovanni Gancitano, Sebia Srl, Florence, Italy.

Supplemental material for this article may be found at http://dx.doi.org/10.1128/IAI.00064-14.

doi:10.1128/IAI.00064-14

The authors have paid a fee to allow immediate free access to this article.

GAS cell division and can mediate bacterial adhesion to epithelial host cells.

MATERIALS AND METHODS

Bacterial strains, growth conditions, and plasmids. The GAS M1-3348, M1-SF370, and M9-2720 strains and culture conditions were previously described (10). The plasmids used to express recombinant proteins in *Escherichia coli* BL21(DE3) (Novagen) were pET21b(+) for the His tag mutants and pET24b(+) for the tagless derivatives. The plasmid pAM-P80 (15) was used for SpyAD expression in *Lactococcus lactis* subsp. *cremoris* MG1363, which was cultured at 30°C with 5% CO_2 in M17 medium (Difco Laboratories) containing 0.5% (wt/vol) glucose (GM17), with 20 μg ml^{-1} chloramphenicol to maintain the episomal plasmid.

***In silico* analysis.** BLASTP search of protein sequence homologies was carried out using the GenBank nonredundant protein database (http://blast.ncbi.nlm.nih.gov/). SignalP server (http://www.cbs.dtu.dk/services/SignalP/) was used for the prediction of signal peptides, COILS (http://embnet.vital-it.ch/software/COILS_form.html), and 2ZIP (http://2zip.molgen.mpg.de/) servers were used to predict the propensity of forming coiled-coil structures, and the TMpred server was used for the prediction of transmembrane regions and orientation (http://embnet.vital-it.ch/software/TMPRED_form.html).

Cloning, expression, and purification of recombinant SpyAD and derivatives. DNA manipulations, including restriction digests, cloning, ligation, and DNA transformation into *E. coli*, were performed according to the manufacturer's recommendations (BioLab Laboratories) and using standard protocols as previously described (16). Plasmid DNA was isolated from *E. coli* with Qiagen plasmid mini- or maxiprep kits (Qiagen) according to the manufacturer's protocol. The oligonucleotides used to clone the recombinant proteins are listed in Table S1 in the supplemental material. Recombinant His-tagged SpyAD and derivatives were expressed in *E. coli* BL21(DE3) cells and purified as previously described (11). Tagless recombinant SpyAD was purified from *E. coli* total cell extracts by two chromatographic steps using Q-Sepharose and butyl Sepharose. Briefly, about 80 to 110 g of bacterial lysate soluble fraction was applied to a 200-ml Q Sepharose XL column (GE Healthcare Biosciences, Piscataway, NJ), equilibrated with 20 mM Tris (pH 8.5). The protein did not bind to the resin, and the flowthrough was collected. Fractions containing SpyAD were pooled and dialyzed against 50 mM Na phosphate (pH 6.8). $(NH_4)_2SO_4$ was added to the pool to a final concentration of 0.45 M, centrifuged for 40 min at 15,000 × *g* (JA14 rotor) to eliminate possible precipitations, and loaded onto a butyl Sepharose 4 FF column (GE Healthcare Biosciences) equilibrated in 0.45 M $(NH_4)_2SO_4$–20 mM Tris (pH 7.0). After a wash with 0.45 M $(NH_4)_2SO_4$, the material bound to the column was eluted with a linear decreasing gradient of $(NH_4)_2SO_4$ from 0.39 M to 60 mM. Fractions containing SpyAD were pooled, dialyzed against phosphate-buffered saline (PBS; pH 7.4), and sterile filtered (0.22 μm pore size). The purified protein was analyzed by sodium dodecyl sulfate-polyacrylamide gel electrophoresis (SDS-PAGE). No contaminants were visible with Coomassie blue staining on gel loading up to 10 μg of sample.

Cytofluorimetric analysis. Cytofluorimetric (FACS) analysis was performed as previously described (11). Essentially, bacteria were grown to mid-log phase, washed twice with PBS, suspended in newborn calf serum (Sigma), incubated for 20 min at room temperature, and dispensed into a 96-well plate (20 μl per well). Then, 80 μl of preimmune or immune mouse serum diluted in PBS–0.1% bovine serum albumin (BSA) was added to the bacterial suspension to a final dilution of 1:200. When the bacterial suspension was incubated with monoclonal antibodies (MAbs), a final concentration of 2 μg ml^{-1} was used. Incubation was performed at 4°C for 30 min. Bacteria were washed, incubated at 4°C for 30 min in 10 μl of goat anti-mouse IgG, and conjugated with $F(ab')_2$ fragment-specific R-phycoerythrin (Jackson ImmunoResearch Laboratories) in PBS–0.1% BSA–20% newborn calf serum to a final dilution of 1:100. Stained bacteria were analyzed with a FACSCanto cytometer (Becton Dickinson) and FlowJo Software. FACS analysis for keratin 1 and collagen VI expression on the cell surface of eukaryotic cell lines was performed using Sigma rabbit anti-collagen VI (SAB4500387) and anti-KRT1 (HPA017917) polyclonal antibodies. Cultured cells were detached from plates by using cell dissociation buffer (Gibco). After a washing step with PBS, the cells were dispensed into a 96-well plate with U-shaped bottoms (2×10^5 cells/well). Serial 2-fold dilutions of anti-keratin 1 and anti-collagen VI were performed in PBS plus BSA 0.5% and added to cells for 1 h at 4°C. After two washes with PBS, the cells were suspended in a PBS plus BSA 0.5% solution with anti-mouse phycoerythrin-conjugated secondary antibody (1:100 [vol/vol]; Jackson ImmunoResearch Laboratories), and incubation was prolonged for 30 min at 4°C. Bound protein was detected using a FACSCanto cytometer, and data were analyzed with FlowJo software.

Generation of specific polyclonal and MAbs. Rabbit sera against SpyAD were obtained by immunizing two New Zealand animals with three 50-μg doses of recombinant protein adjuvanted in alum. Mouse serum anti-SpyAD and anti-FtsZ were obtained by immunizing CD1 mice with three 20-μg doses of recombinant proteins adjuvanted with alum. Mouse MAbs were generated by Areta International (Varese, Italy) according to standard protocols. Briefly, B-cell hybridoma clones were isolated from splenocytes of CD1 mice immunized with the full-length recombinant SpyAD protein. Positive clones were selected by enzyme-linked immunosorbent assay (ELISA) and by Western blotting for binding to SpyAD and its fragments. The selected MAbs were finally purified by protein G affinity chromatography.

Construction of SpyAD mutated strains and analysis of bacterial sedimentation. *SpyAD* in-frame deletion and complementation mutants of GAS M1-3348 strain were constructed as already described (17). Briefly, the in-frame deleted gene product was obtained by splicing-by-overlap-extension PCR (18) using the primers reported in Table S2 in the supplemental material. The amplification product was cloned using BamHI and XhoI restriction sites in the temperature-sensitive shuttle vector pJRS233 (16). Transformation and allelic exchanges were performed as described previously (16, 19, 20). Briefly, the GAS M1-3348 strain was transformed by electroporation, and transformants were selected after growth at 30°C on agar plates containing 1 μg of erythromycin (Sigma) ml^{-1}. Transformants were then grown at 37°C with erythromycin selection. Integrant strains were serially passaged for 5 days in liquid medium at 30°C without erythromycin selection to facilitate the excision of plasmid, resulting in *spyAD* gene deletion on the chromosome. Erythromycin-sensitive colonies were screened by PCR for the absence of the target allele, confirming plasmid excision in the Δ*spyAD* derivative strain. Complementation plasmids were constructed by PCR by using the primers reported in Table S2 in the supplemental material, which allowed the introduction of NotI and BglII restriction sites. The genomic region between the ribosome binding site and the stop codon of *spyAD* gene was amplified, and the PCR product was digested with BamHI and NotI restriction sites and ligated to BglII/NotI-digested pAM401 (21). The *spyAD* gene was inserted into pAM-p80, under the control of the GBS pilus island promoter (15). The expression of the protein SpyAD in the Δ*spyAD*(pAMspyAD) complemented strain was confirmed by cytofluorimetry analysis and immunoblotting on bacterial total cell extracts.

Sedimentation of Δ*spyAD* and of Δ*spyAD*(pAMspyAD) strains was analyzed as already described (22). Briefly, bacteria were grown in Todd-Hewitt broth (THB; Difco Laboratories) overnight at 37°C in 10-ml test tubes. The tubes were gently turned upside down to suspend the bacterial cells. Bacteria were then left to settle at room temperature, and the optical densities at 600 nm (OD_{600}) at various time intervals in the upper half of the tubes were measured to determine the sedimentation rate. Aggregation was also analyzed by microscopy.

Optical and scanning electron microscopy. GAS M1-3348, Δ*spyAD*, and Δ*spyAD*(pAMspyAD) strains were grown in THB at 37°C at an OD_{600} of 0.4. Bacteria were then centrifuged for 10 min at 3,000 × *g* at room temperature and washed in PBS, and drops of bacterial suspensions were

used for the preparation of slides and grids. Slides were observed under an optical microscope with ×63 lens. Grids (Formvar-carbon-coated nickel grids) were fixed in 3% glutaraldehyde in 0.1 M cacodylate buffer (pH 7.3) for 2 h at 4°C. After two washes in sterile water for 30 min each at 4°C, the grids were stained with 1% OsO_4 in 0.1 M cacodylate buffer (pH 7.3) for 1 h at 4°C. After two washes in the same buffer for 30 min each at 4°C, fixed bacteria were dehydrated in 30, 50, 70, 80, 95, and 100% alcohols for 5 min for each change at 4°C. Observation of bacteria was performed by JEOL 1200 EX at 80 kV using a charge-coupled device camera (Megaview; Eloise). Images were imported into Adobe Photoshop and Illustrator CS3 for figure preparation.

Confocal microscopy. To verify SpyAD localization on the cell surface, bacterial cultures of GAS M1-3348, M1-3348Δ*spyAD*, and M9-2720 strains were grown in THB at 37°C to middle logarithmic phase (OD_{600} = 0.4), washed once with PBS, suspended in a half volume of PBS blocking buffer (0.1% BSA–10% normal goat serum [NGS]), and incubated 20 min at room temperature. After a wash with PBS–0.1% BSA, bacteria were incubated at room temperature for 20 min in the same volume of PBS–0.1% BSA with either mouse anti-FtsZ (1:1,500) or rabbit anti-SpyAD (1:500) polyclonal antibodies. After two washes with PBS–0.1% BSA, bacteria were incubated for 15 min at room temperature with secondary antibodies, either goat anti-mouse–Alexa Fluor 568- or anti-rabbit–Alexa Fluor 488-conjugated anti-IgG (Molecular Probes) at 1:1,000. Labeled bacteria were washed twice with PBS–0.1% BSA, suspended in the same volume of PBS–1% formaldehyde, and allowed to adhere to polylysine slides (Thermo Scientific) for 20 min at room temperature. After four washes with PBS, the slides were incubated with biotinylated wheat germ agglutinin (WGA; 1:500)–streptavidin 647 (1:1,000) for 15 min at room temperature, washed three times with PBS, and mounted with ProLong Gold antifade reagent containing DAPI (4′,6′-diamidino-2-phenylindole; Molecular Probes). Images were obtained using a Zeiss LSM 710 confocal microscope (Carl Zeiss).

Immunoprecipitation assay. For coimmunoprecipitation assays, equimolar concentrations (0.42 μM) of FtsZ and SpyAD 33-849 or its fragments were incubated under gentle shaking for 2 h at 22°C in 0.1 M phosphate buffer (pH 7.2). A polyclonal antibody (1:5,000) against either FtsZ or SpyAD was then added to the mixture, followed by incubation overnight at 4°C. The immunocomplex was precipitated by addition of 90 μl of protein A-Sepharose for 45 min at 4°C. Agarose beads were recovered by centrifugation at 11,600 × *g* for 2 min at 4°C, washed three times with phosphate buffer, suspended in 20 μl of Laemmli's sample buffer, and boiled for 5 min. After centrifugation, supernatants were subjected to 12.5% SDS-PAGE, and the proteins were electroblotted onto a nitrocellulose membrane (GE Healthcare), which was blocked with 5% (wt/vol) nonfat dry milk in PBS overnight at 4°C and then incubated for 1 h with anti-SpyAD or anti-FtsZ polyclonal antibodies (1:10,000). After several washes with 0.5% (vol/vol) Tween 20 in PBS (PBST), the membrane was incubated for 45 min with horseradish peroxidase (HRP)-conjugated rabbit anti-mouse IgG. Finally, after additional washes with PBST, the membrane was treated with enhanced chemiluminescence (ECL) detection reagents 1 and 2 according to the procedure recommended by the manufacturer (GE Healthcare) and exposed to an X-ray film for 30 to 60 s.

SpyAD binding to eukaryotic cells. Cultured cells were detached from plates by using enzyme-free Hanks-based cell dissociation buffer (Gibco). After a wash with PBS, the cells were dispensed in a 96-well plate with U-shaped bottoms (2×10^5 cells/well). Serial 2-fold SpyAD dilutions in PBS plus BSA 0.5% were added to cells, and incubation was allowed to proceed for 1 h at 4°C. The cells were then washed twice in PBS, suspended in PBS plus 0.5% BSA containing SpyAD-specific mouse polyclonal antiserum (1:200 [vol/vol]), and incubated at 4°C for 45 min. After two washes with PBS, the cells were suspended in a PBS plus 0.5% BSA solution with anti-mouse phycoerythrin-conjugated secondary antibody (1:100 [vol/vol]; Jackson ImmunoResearch Laboratories), and incubation was prolonged for 30 min at 4°C. Bound protein was detected using a FACSCanto cytometer, and data were analyzed using FlowJo software. The delta mean fluorescence intensity (ΔMFI) of each sample was obtained subtracting from the sample MFI the corresponding value obtained with samples treated with an unrelated polyclonal serum. A Scatchard analysis of the obtained MFI data was used to derive an apparent cell binding affinity (K_d), defined as the concentration determining the saturation of 50% of the receptors present on the cells.

To chemically modify cells surface components, A549 cells were treated as previously described with minor modification (23). For surface proteins, A549 cells were preincubated with pronase (Sigma) or trypsin (Gibco) in fetal calf serum (FCS)-free Dulbecco modified Eagle medium (DMEM) at 37°C in 5% CO_2 for 20 min. For carbohydrates, A549 cells were preincubated with sodium periodate ($NaIO_4$; Sigma) or heparinase I (Sigma) in FCS-free DMEM at 37°C in 5% CO_2 for 1 h. For phospholipids, A549 cells were preincubated with either phospholipase A2 (porcine pancreas; Sigma) or phospholipase C (*Bacillus cereus*; Sigma) in FCS-free DMEM at 37°C in 5% CO_2 for 30 min. After incubation, an equal volume of complete medium was added to each well to stop the reaction of each agent. The cells were subsequently washed and incubated with SpyAD as described above.

ELISA. To evaluate FtsZ binding to immobilized SpyAD or its fragments, SpyAD 33-849 (1 μg/well) or its fragments (0.3 μg/well) in 50 mM sodium carbonate (pH 9.5) were immobilized onto microtiter wells overnight at 4°C. To block additional protein-binding sites, the wells were treated for 1 h at 22°C with 200 μl of 2% BSA in PBS. The plates were then incubated for 1 h with increasing amounts of FtsZ. After extensive washings with PBST, bound protein was detected using an anti-FtsZ mouse antibody (1:10,000) in PBS–0.1% BSA, followed by HRP-conjugated rabbit anti-mouse IgG antibody diluted 1:1,000. After these washings, bound conjugated enzyme was treated with a chromogenic substrate, and the absorbance at 490 nm was determined.

To appraise the binding of recombinant SpyAD to eukaryotic putative ligands, flat-bottom 96-well microtiter plates (MaxiSorp; Nunc) were coated with 10 μg of each human protein/ml (1 μg/well)—keratin 1 (Sigma), fibronectin (Sigma), fibrinogen (Sigma), collagens I, III, IV, and V (Sigma), and collagen VI (Becton Dickinson)—and incubated overnight at 4°C. The wells were washed with PBST buffer and blocked for 2 h at 37°C with 2.7% polyvinylpyrrolidone (PVP) in water. After multiple washings, the plates were incubated with SpyAD serially diluted in PBST–1% BSA and incubated for 2 h at 37°C. To detect binding, the plates were washed, incubated with anti-SpyAD serum in PBST for 1 h and 30 min at 37°C, and then incubated with alkaline phosphatase-conjugated secondary antibody in PBST–1% BSA for 1 h 30 min at 37°C. The wells were developed with 1 mg of *p*-nitrophenyl phosphate (Sigma)/ml in 1 M diethanolamine buffer for 30 min. The reaction was stopped by adding 4 M NaOH, and the absorbance at 405 nm was measured. Wells with PBS only were used as a negative control.

The data were fitted using the following equation: $A = A_{max}\,[L]\,K_a/(1 + K_a\,[L])$, where A is the absorbance at 490 nm, [L] is the molar concentration of ligand, and K_a is the affinity association constant. The apparent dissociation constant (K_d) was calculated as the reciprocal of K_a.

Far-Western blotting. Human keratin 1 (Sigma catalog no. K0253) and collagen VI (Becton Dickinson catalog no. 354261) were separated by using SDS–4 to 12% PAGE under reducing conditions and then electroblotted onto a nitrocellulose membrane using an iBlot dry blotting system (Invitrogen). After blotting, the membranes were incubated with 5% skimmed milk in PBST overnight. To detect keratin 1 and collagen VI, the nitrocellulose membranes were incubated with a polyclonal anti-keratin 1 (Sigma catalog no. HPA017917) and a polyclonal anti-collagen VI antibody (Abcam catalog no. Ab6588), respectively. For far-Western blotting, the membranes were incubated with recombinant SpyAD (5 μg/ml) for 2 h at room temperature. After extensive washing with PBST, the membrane was incubated for 1 h with a rabbit polyclonal anti-SpyAD antibody. After several washes in PBST, the membrane was incubated for 1 h with HRP-conjugated mouse anti-rabbit IgG. Finally, the membrane was

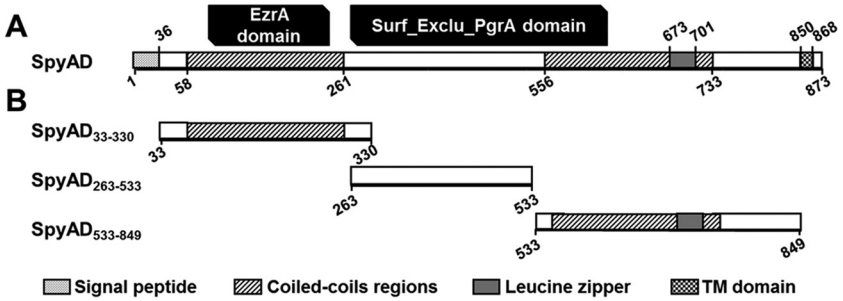

FIG 1 Description of SpyAD protein organization and homologies. (A) Schematic representation of the *spyAD* gene product. The localization of the signal peptide, coiled-coil regions, transmembrane (TM) domains, and leucine zipper motif are shown. Homologies with the EzrA and the PgrA domains are represented by black boxes. The peptide sequences 1 to 32 and 850 to 873 were not included in the SpyAD recombinant protein expressed in *E. coli*. (B) Schematic representation of three SpyAD protein fragments produced in *E. coli* and purified as hexahistidyl-tagged proteins.

treated with ECL detection reagents 1 and 2 according to the procedure recommended by the manufacturer (Bio-Rad) and exposed to an X-ray film for 30 to 60 s.

Heterologous expression of SpyAD and SpyAD/M1 chimera in *L. lactis*. *SpyAD* and *emm1* wild-type sequences were PCR amplified from the GAS M1-3348 strain, and DNA fragments were ligated to pAM-P80 prior transformation into *L. lactis*. *SpyAD*/*emm1* chimera sequences were cloned into pAM-P80 using the polymerase incomplete primer extension cloning method (24). PAM-M1 vector and *spyAD* wild-type sequence were used as the template, and amplification was carried out using the primers listed in Table S3 in the supplemental material. The resulting products were then inserted into *L. lactis* MG1363 competent cells by electroporation, and transformants were selected on GM17 plates with 20 μg chloramphenicol/ml^{-1} and screened by PCR analysis.

***L. lactis* adherence to human epithelial cells *in vitro* and *in vivo*.** Approximately 2×10^5 A549 cells/well were seeded into 24-well culture plates (Nunc), followed by incubation for 24 h at 37°C. *L. lactis* from exponential-phase cultures ($OD_{600} = 0.5$) was collected by centrifugation (3,000 × *g*, 5 min), suspended in DMEM (without serum), and used to infect cell monolayers at 30°C in a 5% CO_2 atmosphere. A multiplicity of infection of 20:1 was used. After 1 h, the wells were extensively washed with PBS to remove unattached bacteria and incubated with 1% saponin to lyse eukaryotic cells, and then the adherent bacteria were plated for enumeration. The average number of bacteria recovered per ml was assessed for each single assay from three independent wells. The experiment was repeated at least three times, and the percentage of adhering bacteria versus the total bacteria was calculated for each time point. Mann-Whitney analysis was used to determine statistically significant adherence rates ($P < 0.05$).

For *in vivo* experiments, 6-week-old female CD1 mice were anesthetized with zoletil and infected intranasally with 2×10^7 to 5×10^7 CFU/mouse (5 μl per nostril). At 24 h after infection, nasal washes were collected and plated on selective agar plates. The data were reported as the recovered CFU per million bacteria inoculated [i.e., ($CFU_{recovered}$/bacterial load) × 10^6]. All animal experiments were approved by Novartis Animal Welfare Body (AWB 201012) and the Italian Ministry of Health (2/2011-B).

RESULTS

***In silico* analysis suggests multiple functions for SpyAD.** SpyAD was initially annotated in the SF370 genome as a "putative surface exclusion protein" for its homology to an *Enterococcus faecalis* plasmid-encoded open reading frame, which regulates cell-to-cell plasmid transfer frequency (25).

The putative protein product of the *spy0269*/*spyAD* gene, as annotated from the M1-SF370 strain, is a conserved polypeptide of 873 amino acids with a molecular mass of 94.7 kDa. The corresponding protein sequence was analyzed *in silico* to highlight any possible motifs and homologies to known bacterial proteins. We predicted a signal peptide with a proposed cleavage site between residues alanine 36 (A36) and aspartic acid 37 (D37). No typical cell wall anchoring (LPXTG) motif shared by surface-anchored proteins of Gram-positive bacteria was deduced at the C terminus, although a putative hydrophobic transmembrane domain followed by a charged tail was identified (residues 850 to 873). Secondary structure predictions indicated a high probability of coiled-coil arrangements in protein regions 58 to 261 and 554 to 721, the latter including a leucine zipper motif between residues L673 and L701 (Fig. 1A).

Among the homologies with other bacterial proteins found by BLASTP analysis, three appeared particularly intriguing to us. A short SpyAD stretch (residues 96 to 228) exhibited some degree of similarity with a domain of EzrA from *Bacillus subtilis* (26), an interactor of FtsZ regulating the bacterial division system. In addition, SpyAD exhibited partial homology to reported adhesins from other streptococcal species: the *Streptococcus uberis* adhesion protein SUAM (39% identity, 58% positivity along the full amino acid sequence), known to mediate adhesion to mammary epithelial cells, and the *Streptococcus equi* subsp. *equi* 4047 membrane protein SEQ_0339 (51% identity, 67% positivity) (27), containing the Se89.9 fragment that strongly binds to the stratified squamous epithelium of the equine lingual tonsil, a point of entry of *S equi* (J. F. Timoney, unpublished data). SpyAD's relationship to these and other streptococcal proteins extended to secondary structure predictions of coiled-coil arrangements (see Fig. S1 in supplemental material), as well as to the genomic context in which the corresponding gene appeared to be located (see Fig. S2 in supplemental material). In fact, *spyAD* and its homologous genes were found between the conserved *purR* and *rpsL* sequences in *S. pyogenes*, *S. uberis*, *S. dysgalactiae*, *S. equi*, and *S. zooepidemicus*. Interestingly, no DNA sequences were found between *purR* and *rpsL* in the evolutionary close *S. agalactiae*, whereas large genomic regions were found between *purR* and *rpsL* in *S. suis* and *S. pneumoniae*.

Deletion of the *spyAD* gene affects the capacity of GAS to properly divide. Searching for a phenotype which could possibly indicate a SpyAD function, we generated an isogenic deletion mutant in the GAS M1-3348 strain (Δ*spyAD*) in which the protein was not expressed, as confirmed by Western blotting and cytofluorimetric analysis (see Fig. S3 in the supplemental material).

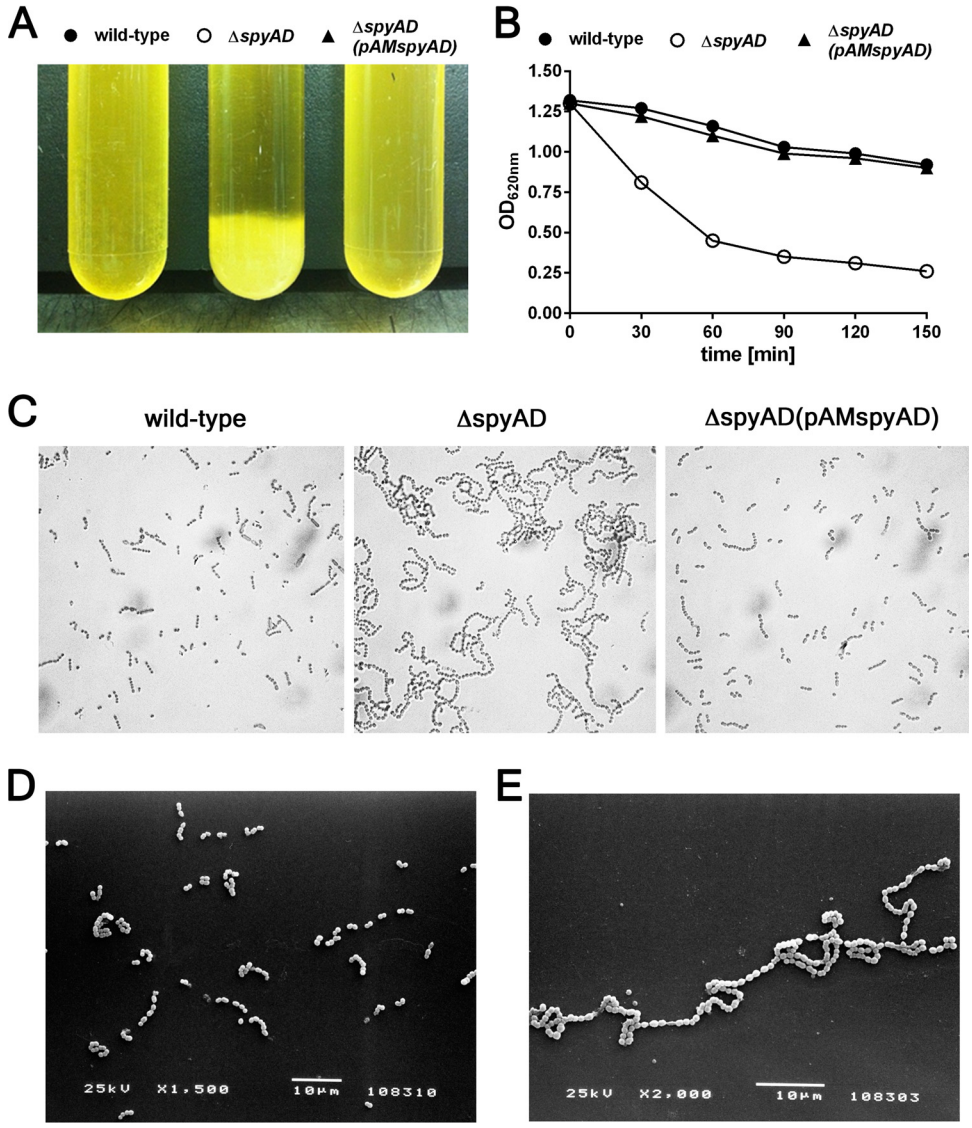

FIG 2 Analysis of *spyAD* deletion mutant (Δ*spyAD*) bacterial cultures. (A) Bacterial cultures of GAS M1-3348 wild-type strain, *spyAD* gene deletion mutant (Δ*spyAD*), and *spyAD* complemented strains Δ*spyAD*(pAMspyAD) observed after 150 min of incubation. (B) Schematic representation of the sedimentation rate curves of the three strains, obtained by measuring the 620-nm optical densities in the upper part of the tubes at different time points. (C) Representative images of the three strains obtained by optical microscopy (high-contrast digital enhancement). (D and E) Representative images obtained by scanning electron microscopy of the GAS M1-3348 wild-type strain and the Δ*spyAD* gene deletion mutant, respectively.

As shown in Fig. 2A and B, the strain showed visible sedimentation in cell culture tubes and a higher sedimentation rate compared to wild type. Optical and scanning electron microscopy revealed the formation of shorter chains by the wild-type strain compared to the *spyAD* knockout mutant, which formed much longer chains (Fig. 2C, D, and E) that could possibly enhance the formation of aggregates and the observed sedimentation. This phenotype appeared to be specific since it was reverted by transforming the M1-3348 knockout strain with an episomal vector overexpressing SpyAD (Fig. 2A, B, and C).

This experimental evidence, along with the observed homology with EzrA, suggested that SpyAD could be involved in the cell division/separation process, possibly interacting or affecting the function of proteins that are part of the divisome machinery. As previously reported (28–30), the depletion of proteins involved in the cell division/separation process in both Gram-positive and Gram-negative bacteria produces a phenotype very similar to that observed with the *spyAD* knockout strain.

SpyAD colocalizes with the cell division protein FtsZ at the bacterial septum. Since the localization at the cell septum is a prerequisite of proteins involved in the division process, we investigated the localization of SpyAD on the bacterial cell surface. GAS M1-3348 and its derived Δ*spyAD* mutant strain were grown to mid-logarithmic phase and analyzed by confocal microscopy using anti-SpyAD rabbit serum and biotinylated WGA lectin to reveal the cell wall peptidoglycan and DAPI to stain nuclei. SpyAD appeared mainly localized at the bacterial septum (Fig. 3A), whereas no staining was observed for the Δ*spyAD* mutant strain used as negative control (Fig. 3B). When SpyAD expression was restored by complementing the mutation with a plas-

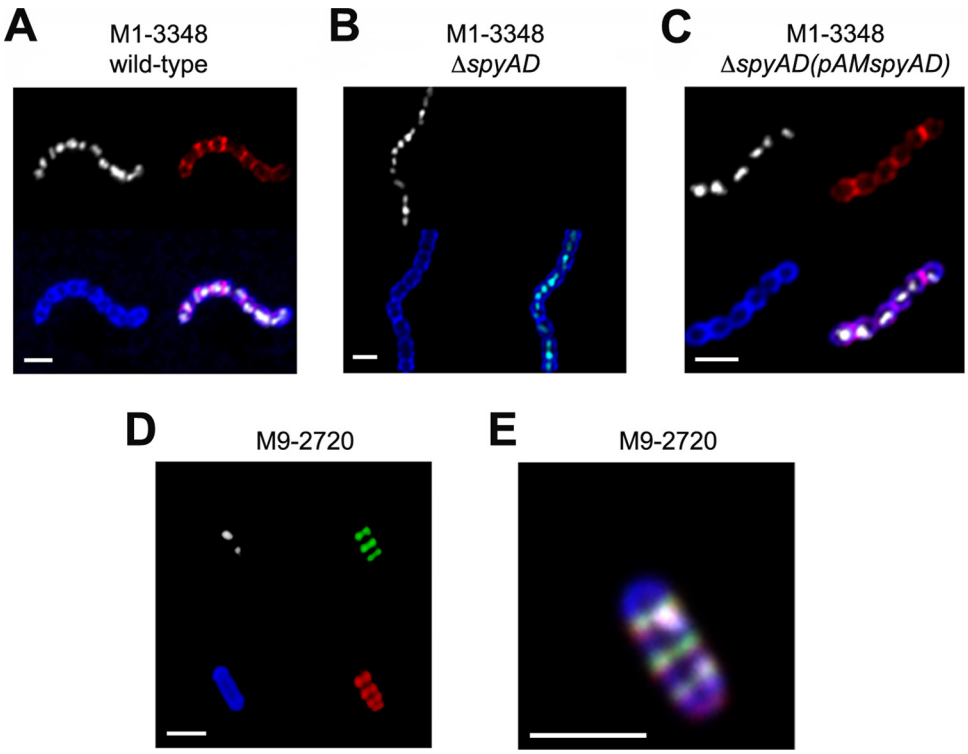

FIG 3 SpyAD cellular localization analysis. (A to C) The GAS M1-3348 wild-type strain (A), Δ*spyAD* deletion mutant (B), and *spyAD* complemented strain (C) were stained with specific SpyAD rabbit antiserum and secondary goat anti-rabbit antibodies (red), with biotinylated WGA for cell wall peptidoglycan (blue), and with DAPI for nuclei (white). Merging of the three images is shown in the lower right position of each panel. (D) GAS M9-2720 stained as in panel A but with anti-FtsZ mouse antibodies detected by secondary anti-mouse antibodies (green). (E) Merged image of the four images reported in panel D.

mid (pAM) carrying the *spyAD* gene, staining at the septum was restored (Fig. 3C).

To further support these observations, we compared the cellular localization of SpyAD to that of the cell division protein FtsZ for which septal localization has already been reported in other bacterial species. Colocalization of SpyAD and FtsZ at the cell septum of M9-2720, a strain that expresses large amounts of SpyAD, was investigated by confocal microscopy using rabbit anti-SpyAD and mouse anti-FtsZ specific antibodies. As shown in Fig. 3D and E, we observed overlapping fluorescent signals at the incipient division sites, confirming colocalization. Overall, the obtained data reinforced the hypothesis that SpyAD could be involved in the bacterial cell division process, possibly modulating the GAS divisome machinery.

SpyAD directly interacts with FtsZ *in vitro*. Having demonstrated that SpyAD colocalizes with FtsZ at the bacterial cell septum, we sought to investigate whether the two proteins could form a molecular complex *in vitro*. Full-length FtsZ and SpyAD (from amino acids 33 to 849, excluding the putative signal peptide and C-terminal transmembrane domains; Fig. 1A) were purified as soluble recombinant proteins. Equimolar concentrations of the two proteins were coincubated in the presence of polyclonal antibodies raised against either FtsZ or SpyAD, and the immunocomplexes were precipitated by addition of protein A/G-agarose beads. Coimmunoprecipitation of SpyAD and FtsZ by antibodies specific against either of the two proteins was confirmed by immunoblotting (Fig. 4A and B, lanes 1, and Fig. 4C and D). As a control, coincubation of FtsZ with a different *S. pyogenes* surface protein (SpyCEP) did not result in any signal detection when the immunoprecipitate was subjected to Western blotting with anti-SpyCEP antibodies (data not shown). These data suggested a specific interaction between FtsZ and SpyAD under *in vitro* conditions.

To further dissect the SpyAD binding capacity toward FtsZ, three fragments of the protein were obtained as His-tagged fusions (Fig. 1B): N-terminal (amino acids 33 to 330) and C-terminal (amino acids 533 to 849) portions with propensity to form coiled-coil structures, as well as the internal region from amino acids 263 to 533. When the three purified SpyAD protein fragments were investigated in immunoprecipitation experiments, only the C-terminal domain was shown to interact with FtsZ, whereas no interactions were observed with the N-terminal or the internal regions (Fig. 4A and B, lanes 2 to 4).

The interaction was further confirmed by immobilizing recombinant SpyAD or its fragments onto microtiter wells, followed by probing with increasing concentrations of FtsZ, and detection of complex formation with anti-FtsZ IgG. As shown in Fig. 4E, dose-dependent interactions with half maximal binding concentrations (K_d) of $(2.2 \pm 0.3) \times 10^{-7}$ M and $(1.0 \pm 0.1) \times 10^{-7}$ M were revealed for SpyAD and C-terminal SpyAD, respectively, whereas no binding was observed for the N-terminal and internal fragments. The data further confirmed a possible role of SpyAD in the *S. pyogenes* cell division process.

FtsZ has been reported as cytosolic in several bacterial species, but confocal results showing that it can be stained by specific antibodies suggested that in the case of GAS this protein can be

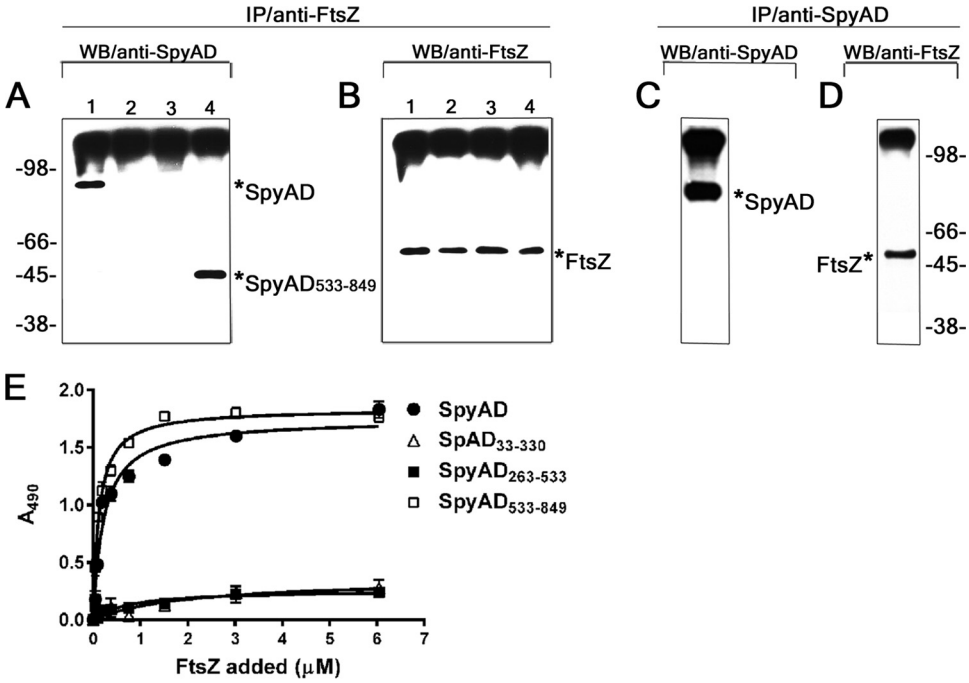

FIG 4 Analysis of the interaction between recombinant SpyAD and FtsZ. Western blot analysis of coincubated FtsZ and SpyAD immunoprecipitated with either FtsZ-specific (A and B) or SpyAD-specific (C and D) antisera (indicated as IP) and probed with anti-SpyAD (A and C) or anti-FtsZ (B and D) antibodies (indicated as WB) was performed. FtsZ was coincubated with full-length SpyAD (panels A and B, lanes 1, and panels C and D) or its three fragments ($SpyAD_{33-330}$ [lanes 2], $SpyAD_{263-533}$ [lanes 3], and $SpyAD_{533-849}$ [lanes 4] in panels A and B). (E) Dose-dependent binding of FtsZ to SpyAD. SpyAD and the three protein fragments were immobilized onto microtiter wells and incubated with increasing amounts of FtsZ; binding was detected using anti-FtsZ and conjugated secondary antibodies. The absorbance was measured at 490 nm (A_{490}).

exposed on the bacterial surface. Surface exposure of FtsZ was further confirmed by FACS analysis of GAS M1-3348, its *spyAD* deletion mutant, and M9-2720 strains using anti-FtsZ antibodies (see Fig. S4A in the supplemental material). Confocal microscopy experiments comparing wild-type and Δ*spyAD* M1-3348 strains indicated identical FtsZ surface exposure and septal localization in presence or absence of SpyAD (see Fig. S4B in the supplemental material).

Recombinant SpyAD binds to mammalian epithelial cells. *In silico* analysis indicating that SpyAD had homology with reported adhesins and flow cytometry data showing high exposure on the bacterial cell surface led us to hypothesize a second possible role of this protein in mediating GAS interaction with host cells. Cytofluorimetric analysis was used to test whether recombinant SpyAD could bind to human epithelial cells *in vitro*. As shown in Fig. 5A, SpyAD was able to bind to A549 human pulmonary epi-

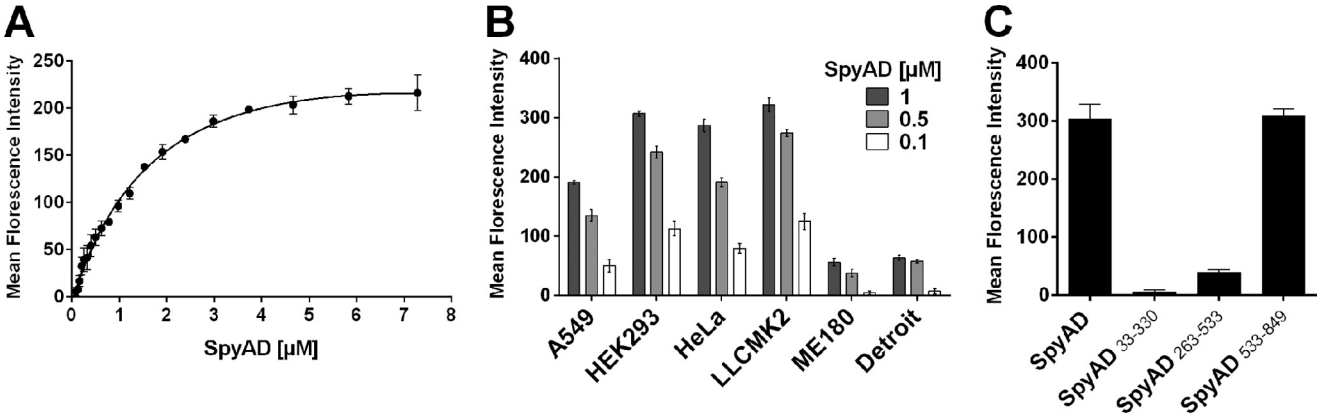

FIG 5 Recombinant SpyAD binding to human epithelial cells. (A) Saturation curve of SpyAD binding to A549 cells. Cells were incubated for 1 h at 4°C with increasing concentrations of recombinant SpyAD from 0.08 to 7.28 μM (*x* axis). Binding was detected using mouse anti-SpyAD and phycoerythrin-conjugated secondary antibodies, followed by flow cytometry analysis (the mean fluorescence intensity is reported on the *y* axis). (B) Bar graph showing binding of SpyAD to different human and mammalian epithelial cell lines. The mean fluorescence intensity obtained for each cell line with three different SpyAD concentrations (1 μM, dark gray bars; 0.5 μM, light gray bars; 0.1 μM, white bars) is reported on the *y* axis. (C) Binding of the three SpyAD protein fragments to A549 cell line. Cells were incubated for 1 h at 4°C with an equimolar concentration of each recombinant fragment (2.5 μM), and binding was measured by flow cytometry as reported above.

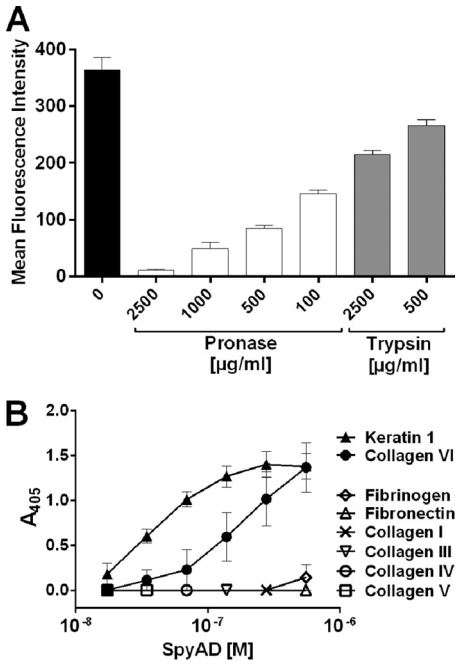

FIG 6 Biochemical characterization of SpyAD binding to epithelial cells. (A) A549 cells were treated with either medium alone (black bar) or with the indicated concentrations of pronase (white bars) or trypsin (gray bars), prior to incubation with recombinant SpyAD (1 μM). SpyAD binding to the treated cells was analyzed by flow cytometry using an anti-SpyAD antiserum, and the mean fluorescence intensity was measured (*y* axis). (B) Graph showing the interaction of SpyAD with immobilized human proteins. ELISA plates were coated with 10 μg of fibrinogen, fibronectin, keratin 1, or collagens I, III, IV, V, or VI ml^{-1}, followed by incubation with serial dilutions of recombinant SpyAD protein (5.5×10^{-7} to 1.7×10^{-8} M). Binding of the protein was detected by using anti-SpyAD and alkaline phosphatase-conjugated-secondary antibodies. Mean values and standard error bars from three experiments are shown.

thelial cells in a dose-dependent manner, and binding could be saturated with an apparent equilibrium dissociation constant (K_d) of approximately 8×10^{-7} M. Binding to other mammalian epithelial cell lines was also investigated, demonstrating that the protein could consistently bind to HEK293, HeLa, and LLCMK2 cells and, to a lesser extent, to ME180 and Detroit cells (Fig. 5B).

To gain additional information on the SpyAD protein region involved in the binding to a putative cell receptor, the three previously described protein fragments were tested for their capacity to interact with A549 cells. As shown in Fig. 5C, only the C-terminal fragment could bind to cells. BLASTP analysis of this fragment versus the previously mentioned SUAM adhesin and the Se89.9 adhesive fragment of the membrane protein SEQ_0339 indicated sequence identity levels of 30 and 49%, respectively, which were similar to those obtained comparing the full-length proteins.

To investigate the chemical nature of the SpyAD putative cellular receptor, A549 cells were treated with different concentrations of multicomponent proteolytic enzymes (pronase) or with trypsin prior to binding to recombinant SpyAD. Pronase treatment could reduce or completely abolish SpyAD interaction in a dose-dependent manner, whereas trypsin partially decreased SpyAD binding (Fig. 6A). Heparinase II, phospholipases A2 and C, and sodium periodate did not affect cell adhesion (data not shown), suggesting that glycosaminoglycans, phospholipids, and carbohydrate do not mediate SpyAD binding to epithelial cells, although involvement of a carbohydrate ligand cannot be entirely excluded since the periodate reaction requires vicinal hydroxyl groups, which may not be present in the SpyAD ligand binding region. We subsequently tested the capacity of SpyAD to interact with eukaryotic ligands of bacterial adhesins. *In vitro* binding assays were performed on microtiter plates coated with fibrinogen, fibronectin, keratin 1, and various types of collagen as target molecules, and the binding extent was quantified by using a specific SpyAD polyclonal rabbit antiserum. Recombinant SpyAD appeared to bind to human keratin 1 and collagen VI (Fig. 6B). No significant binding of SpyAD to human fibrinogen, fibronectin, and collagen types I, III, IV, and V was detected.

Binding specificity of SpyAD to keratin 1 and collagen VI was also assessed by Far-Western blotting. This analysis confirmed that SpyAD bound to a protein migrating on SDS-PAGE accordingly with the reported molecular weight for keratin 1 and recognized by an anti-keratin 1 specific antibody (see Fig. S5A and B in the supplemental material). Binding of SpyAD to the bands corresponding to denatured alpha subunits of collagen VI was not apparent, but staining was visible for a higher-molecular-weight species (see Fig. S5C and D in the supplemental material). This high-molecular-weight material, also recognized by anti-collagen VI antibodies, possibly represents nonreduced cross-linked collagen VI (31, 32). The data suggest that SpyAD binds preferably to nondenatured collagen VI organized in high-level structures. As shown in Fig. S5D, lane 2, in the supplemental material, no binding to the fibronectin used as a negative control was detected.

FACS analysis using collagen VI specific antibodies confirmed high exposure of collagen VI on the surface of all cell lines tested for SpyAD binding (see Fig. S6 in the supplemental material). No signals were instead obtained using anti-keratin 1 antibodies in the investigated experimental conditions. However, we cannot rule out greater accessibility *in vivo* during infections and other inflammatory conditions that may significantly alter epithelial integrity or during repair and remodeling of epithelial surfaces. Overall, the data suggest that a protein ligand is likely to mediate binding of SpyAD to epithelial cells through a direct protein-protein interaction and that collagen VI and keratin 1 are two potential receptors.

Expression of SpyAD in *L. lactis* mediates cell adhesion *in vitro* and *in vivo*. Comparative cell binding assays using the wild-type M1-3348 strain and its Δ*spyAD* derivative to definitely confirm the role of SpyAD in GAS cell adhesion could not be undertaken due to the phenotype exhibited by the knockout strain, which prevented precise bacterial counting.

To overcome this drawback, we expressed SpyAD in the heterologous bacterial host *Lactococcus lactis* (33, 34). This nonpathogenic bacterium does not significantly adhere to human epithelial cells but is capable of efficiently expressing and exporting functional exogenous proteins to the cell surface (15, 35). Expression of wild-type SpyAD was obtained in *L. lactis* MG1363 using the pAM episomal vector in which protein synthesis is driven by the strong P80 promoter from *Streptococcus agalactiae* (15). Figure 7A shows that the expression of wild-type SpyAD in *L. lactis* resulted only in a partial shift of bacterial fluorescence after staining with anti-SpyAD polyclonal antibodies (central panel) compared to the negative-control strain containing the empty vector only (left panel). Low expression could possibly be due to inefficient recognition of SpyAD by the *L. lactis* secretion/anchoring machineries.

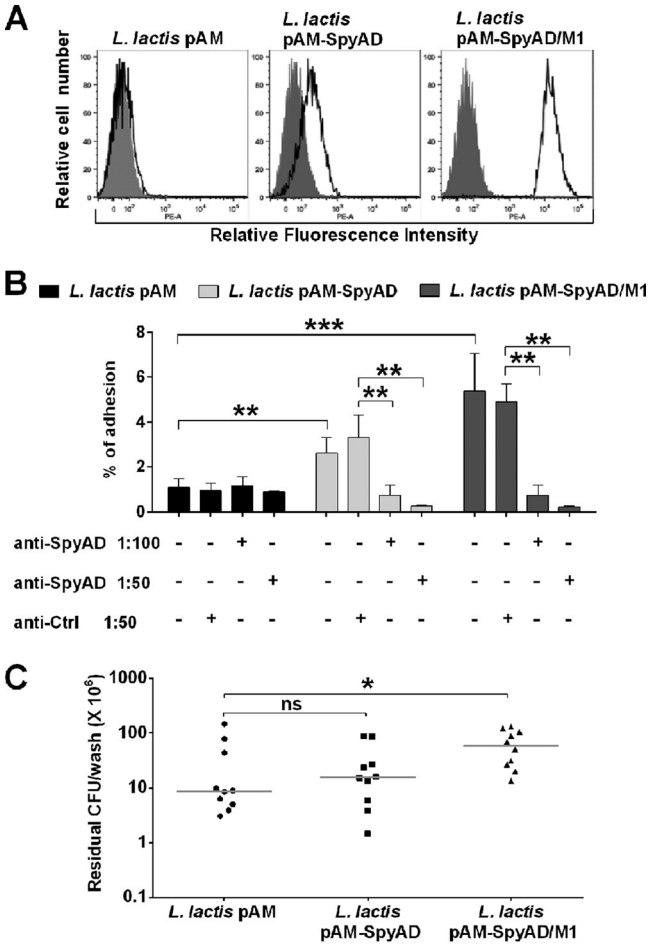

FIG 7 *In vitro* and *in vivo* cell adhesion of *L. lactis* expressing SpyAD. (A) Flow cytometry analysis of *L. lactis* expressing either full-length SpyAD (pAM-SpyAD) or the SpyAD/M1 chimera (pAM-SpyAD/M1) compared to a strain carrying the vector alone (pAM). Filled and empty histograms indicate staining of bacteria with a serum raised against alum adjuvant alone and with a polyclonal mouse SpyAD antiserum, respectively. (B) Bar graph showing *in vitro* adhesion of the three *L. lactis* strains to A549 human epithelial cells and specific inhibition of the binding by anti-SpyAD antibodies. The percentage of adhesion of *L. lactis* to A549 cells is reported on the *y* axis. Serum dilutions tested for the inhibition of cell binding are reported below the *x* axis. Black, light gray, and dark gray bars illustrate the results obtained when cells were incubated with the pAM, pAM-SpyAD, and SpyAD/M1 *L. lactis* strains, respectively (the multiplicity of infection was 20:1). Means and standard deviations from six to eight experiments are represented. Statistical significance: **, $P < 0.01$; ***, $P < 0.001$. (C) *In vivo* adhesion of the three recombinant *L. lactis* strains to the nasal mucosa of CD1 mice. The strains used to infect mice intranasally (2×10^7 to 5×10^7 CFU/mouse) are indicated on the *x* axis. The *y* axis reports the number of recovered CFU per million bacteria inoculated by performing nasal washes 20 h after infection. *, $P < 0.05$; ns, not significant.

To obtain a *L. lactis* strain highly expressing SpyAD, we attempted to obtain a recombinant protein fusion derivative containing the export and anchoring signals of the *S. pyogenes* M1, a strategy previously used for other heterologous proteins (36–39). The recombinant SpyAD/M1 chimera was obtained by replacing both the SpyAD signal peptide and C-terminal putative transmembrane domain sequences with the M1 leader peptide and cell wall anchoring sequences, respectively. As shown in the right panel of Fig. 7A, the SpyAD/M1 chimera was highly exposed on the cell surface of *L. lactis*. Furthermore, FACS analysis with MAbs directed against different SpyAD regions showed a similar reaction pattern on wild-type M1-3348 and on *L. lactis* expressing both the original SpyAD sequence and the SpyAD/M1 chimera (see Fig. S7 in the supplemental material), suggesting that the conformation of the exposed chimera was not significantly altered.

To demonstrate that *Lactococcus* surface-localized SpyAD mediated bacterial binding to cells, recombinant strains expressing either SpyAD or the protein chimera were tested *in vitro* and *in vivo*. A549 cells monolayers were infected with the *L. lactis* derivative strains, and the percentage of cell-associated CFU versus the total bacterial input was estimated (Fig. 7B). *L. lactis* strains expressing the two forms of SpyAD appeared to significantly adhere to A549 cells, as opposed to *L. lactis* containing the episomal expression vector only. *L. lactis* expressing the SpyAD/M1 chimera had the highest adhesion rate, a finding consistent with the higher cell surface exposure of the protein. The specificity of SpyAD-mediated adhesion was confirmed by binding inhibition experiments showing that anti-SpyAD purified IgG was able to prevent binding of the recombinant strains to A549 cells.

Finally, to investigate whether SpyAD could mediate adhesion *in vivo*, CD1 mice were infected intranasally with the *L. lactis* strains expressing either the wild-type antigen or the SpyAD/M1chimera. Bacterial recovery from nasal washes 20 h after infection demonstrated a higher number of CFU in animals infected with *L. lactis* expressing SpyAD compared to control bacteria containing the empty vector. Statistically significant differences could be attained in mice infected with the SpyAD/M1 chimera versus the negative control (Fig. 7C).

DISCUSSION

The conserved, surface-associated GAS antigen Spy0269, here renamed *Streptococcus pyogenes* Adhesion and Division protein, or SpyAD, elicits a prominent protective immune response in mouse models of GAS infection (10, 40, 41). The data presented here suggest that SpyAD contributes to both bacterial division and adhesion to host cells. The ability of some proteins to exert more than one biological function is well described both in eukaryotes and in prokaryotes, and several "moonlighting" proteins have been identified in a wide range of human pathogens, including group A streptococcus. Among them, glyceraldehyde-3-phosphate dehydrogenase (GAPDH), enolase, chaperonin 60, Hsp70, and peptidyl prolyl isomerase are known bacterial moonlighting proteins playing a role in bacterial virulence (42–44).

The striking long-chain phenotype observed when the *spyAD* gene was deleted, as well as the evidence showing that GAS SpyAD is localized in the bacterial septum and that a recombinant version of the protein can interact with FtsZ, strongly suggested that SpyAD is involved in the process(es) leading to cell division.

A common theme in bacterial cell division is the initial polymerization of the tubulin homolog FtsZ into a Z-ring, followed by recruitment of additional proteins that assemble into the divisome. This large macromolecular complex is constituted of cytosolic and membrane components that were recently shown to incorporate both the cell division apparatus and the peptidoglycan synthesis machinery (45, 46). FtsZ polymerization into the Z-ring provides a driving force to constrict the plasma membrane of the parent cell at the equatorial level, resulting in the formation of two equal daughter cells. EzrA, with which SpyAD showed partial homology, was first identified in *B. subtilis* as a negative regulator of Z-ring assembly that enhances FtsZ GTP hydrolysis and depoly-

merization, thus controlling cell division dynamics to maintain correct cell size (26, 47). EzrA was also shown to positively regulate cell elongation by interacting with the penicillin-binding protein PBP1 (48), and its expression levels and multiple interactions with the divisome machinery components determine distinct roles in the *S. aureus* cell division process (49). The precise role of SpyAD in cell division was not determined in the present study and will be the subject of our future studies. Recent investigations have clearly indicated that the divisome of *E. coli* (50), *S. pneumoniae* (51), and *S. aureus* (49) are built by a complex network of interactions where each component interacts with multiple partners. By homology search, we identified the GAS counterpart of most genes involved in division of *S. pneumoniae* (see Table S4 in the supplemental material) and we predict that, in addition to FtsZ, SpyAD possibly interacts with other components of the GAS cell division apparatus and/or the peptidoglycan synthesis machinery located in the septum of Gram-positive cocci (52, 53). Indeed, SpyAD shares structural features of many divisome interacting proteins including coiled-coil arrangements and a leucine zipper motif.

A second possible role of SpyAD as a novel GAS adhesin was evidenced by its capacity to bind to eukaryotic cells *in vitro* and to mediate bacterial adhesion to the nasal epithelium *in vivo*. SpyAD could adhere to different epithelial cell lines and also to human brain microvascular endothelial cells (data not shown). The absence of strict cell type specificity is not unexpected, since GAS and other streptococci have a large pool of molecules that mediate host cell adhesion with various affinities (6, 7). A two-step mechanism has been proposed for GAS cell adhesion according to which an initial weak and reversible contact with host cells is followed by a second adhesion step mediated by different arrays of adhesins, which confer cell and tissue specificity (54). We hypothesize that SpyAD may interact with the host at a stage of infection in which a weak and low specific adhesion is required, possibly binding to cellular surface-exposed proteins or the extracellular matrix. *In vitro* binding experiments to eukaryotic cell proteins actually indicated that SpyAD can bind to human collagen VI and keratin 1. Collagen VI is localized in vascular walls and in the interstitial space of the upper and lower airways, beneath the basement membrane of the epithelium, and is a target for streptococcal adhesins, including *S. pyogenes* M protein (55). Keratin 1 and its heterodimer type I partner, keratin 10, are major components of the cytoskeleton in suprabasal keratinocytes of the stratified squamous epithelia (56). Keratin 1 is also present on the cell surfaces of endothelial cells (57). We can envisage that infections and other inflammatory conditions may significantly alter epithelial integrity, leading to partial or complete shedding of epithelial basal cells and lamina and unmasking of potential receptors for bacterial adhesion (58, 59). This scenario would fit well with the fact that GAS readily colonizes the nasal and upper respiratory tract epithelia, tissues that frequently undergo tissue repair and remodeling.

The assignment of distinct roles to SpyAD raised the intriguing question regarding how this protein is able to interact both with host cell ligands and with FtsZ, which was reported as cytoplasmic in several bacterial species (45, 46). However, *in silico* analysis of GAS FtsZ using different topological prediction software (e.g., TMpred) indicated the presence of both cytosolic and extracellular domains. FACS results and confocal microscopy confirmed that both SpyAD and FtsZ are exposed on the surface of *S. pyogenes*. The data are consistent with previous evidence indicating that FtsZ-derived peptides could be obtained by "surfome" analysis of live GAS SF370, where live bacteria were treated with proteases, and the peptides released from surface exposed proteins were analyzed by mass spectrometry (11). Other examples of FtsZ homologs present on the bacterial surface include the cell division protein of *Bartonella bacilliformis* containing a C-terminal region that was shown to be immunogenic and surface exposed (60). This experimental background confirms that SpyAD localization is compatible with interactions with both FtsZ and host cell ligands. In this context, the SpyAD C terminus (316 amino acids) may be sufficiently long to mediate in due time two different interaction types.

In conclusion, based on the evidence reported in the present study, we predict that induction of functional antibodies against SpyAD can impair the capacity of the pathogen to properly divide and colonize specific host niches. This may contribute to the observed SpyAD-mediated highly protective immune response in mouse models of infection, which makes this antigen an excellent candidate for a multicomponent broadly effective vaccine against group A streptococcus.

ACKNOWLEDGMENTS

We thank Francesco Berti, Fabiana Falugi, Laura Ciucchi, Paolo Ruggiero, and Sabrina Capo for their support.

This study was supported by internal funding from Novartis NVD and by the Italian Ministry of Instruction, University and Research, Rome, Italy (MIUR grant 10911).

REFERENCES

1. **Bisno AL, Brito MO, Collins CM.** 2003. Molecular basis of group A streptococcal virulence. Lancet Infect. Dis. **3:**191–200. http://dx.doi.org/10.1016/S1473-3099(03)00576-0.
2. **Cunningham MW.** 2000. Pathogenesis of group A streptococcal infections. Clin. Microbiol. Rev. **13:**470–511. http://dx.doi.org/10.1128/CMR.13.3.470-511.2000.
3. **Cunningham MW.** 2008. Pathogenesis of group A streptococcal infections and their sequelae, p 29–42. *In* Finn A, Pollard A (ed), Hot topics in infection and immunity in children IV. Springer, New York, NY.
4. **Tart AH, Walker MJ, Musser JM.** 2007. New understanding of the group A streptococcus pathogenesis cycle. Trends Microbiol. **15:**318–325. http://dx.doi.org/10.1016/j.tim.2007.05.001.
5. **Bessen DE, Lizano S.** 2010. Tissue tropisms in group A streptococcal infections. Future Microbiol. **5:**623–638. http://dx.doi.org/10.2217/fmb.10.28.
6. **Courtney HS, Hasty DL, Dale JB.** 2002. Molecular mechanisms of adhesion, colonization, and invasion of group A streptococci. Ann. Med. **34:**77–87. http://dx.doi.org/10.1080/07853890252953464.
7. **Nobbs AH, Lamont RJ, Jenkinson HF.** 2009. *Streptococcus* adherence and colonization. Microbiol. Mol. Biol. Rev. **73:**407–450. http://dx.doi.org/10.1128/MMBR.00014-09.
8. **Steer AC, Batzloff MR, Mulholland K, Carapetis JR.** 2009. Group A streptococcal vaccines: facts versus fantasy. Curr. Opin. Infect. Dis. **22:**544–552. http://dx.doi.org/10.1097/QCO.0b013e328332bbfe.
9. **Dale JB, Fischetti VA, Carapetis JR, Steer AC, Sow S, Kumar R, Mayosi BM, Rubin FA, Mulholland K, Hombach JM, Schödel F, Henao-Restrepo AM.** 2013. Group A streptococcal vaccines: paving a path for accelerated development. Vaccine **31**(Suppl 2)**:**B216–B222.
10. **Bensi G, Mora M, Tuscano G, Biagini M, Chiarot E, Bombaci M, Capo S, Falugi F, Manetti AGO, Donato P, Swennen E, Gallotta M, Garibaldi M, Pinto V, Chiappini N, Musser JM, Janulczyk R, Mariani M, Scarselli M, Telford JL, Grifantini R, Norais N, Margarit I, Grandi G.** 2012. Multi-high-throughput approach for highly selective identification of vaccine candidates: the group A *Streptococcus* case. Mol. Cell. Proteomics **11:**M111.015693. http://dx.doi.org/10.1074/mcp.M111.015693.
11. **Rodriguez-Ortega MJ, Norais N, Bensi G, Liberatori S, Capo S, Mora M, Scarselli M, Doro F, Ferrari G, Garaguso I, Maggi T, Neumann A, Covre A, Telford JL, Grandi G.** 2006. Characterization and identification

of vaccine candidate proteins through analysis of the group A streptococcus surface proteome. Nat. Biotechnol. **24:**191–197. http://dx.doi.org/10.1038/nbt1179.

12. **Chiarot E, Faralla C, Chiappini N, Tuscano G, Falugi F, Gambellini G, Taddei A, Capo S, Cartocci E, Veggi D, Corrado A, Mangiavacchi S, Tavarini S, Scarselli M, Janulczyk R, Grandi G, Margarit I, Bensi G.** 2013. Targeted amino acid substitutions impair streptolysin O toxicity and group A streptococcus virulence. mBio **4:**e00387-12. http://dx.doi.org/10.1128/mBio.00387-12.
13. **Kurupati P, Turner CE, Tziona I, Lawrenson RA, Alam FM, Nohadani M, Stamp GW, Zinkernagel AS, Nizet V, Edwards RJ, Sriskandan S.** 2010. Chemokine-cleaving *Streptococcus pyogenes* protease SpyCEP is necessary and sufficient for bacterial dissemination within soft tissues and the respiratory tract. Mol. Microbiol. **76:**1387–1397. http://dx.doi.org/10.1111/j.1365-2958.2010.07065.x.
14. **Bombaci M, Grifantini R, Mora M, Reguzzi V, Petracca R, Meoni E, Balloni S, Zingaretti C, Falugi F, Manetti AGO, Margarit I, Musser JM, Cardona F, Orefici G, Grandi G, Bensi G.** 2009. Protein array profiling of Tic patient sera reveals a broad range and enhanced immune response against group A streptococcus antigens. PLoS One **4:**e6332. http://dx.doi.org/10.1371/journal.pone.0006332.
15. **Buccato S, Maione D, Rinaudo CD, Volpini G, Taddei AR, Rosini R, Telford JL, Grandi G, Margarit I.** 2006. Use of *Lactococcus lactis* expressing pili from group B streptococcus as a broad-coverage vaccine against streptococcal disease. J. Infect. Dis. **194:**331–340. http://dx.doi.org/10.1086/505433.
16. **Perez-Casal J, Price JA, Maguin E, Scott JR.** 1993. An M protein with a single C repeat prevents phagocytosis of *Streptococcus pyogenes*: use of a temperature-sensitive shuttle vector to deliver homologous sequences to the chromosome of *S. pyogenes*. Mol. Microbiol. **8:**809–819. http://dx.doi.org/10.1111/j.1365-2958.1993.tb01628.x.
17. **Mora M, Bensi G, Capo S, Falugi F, Zingaretti C, Manetti AGO, Maggi T, Taddei AR, Grandi G, Telford JL.** 2005. Group A streptococci produce pilus-like structures containing protective antigens and Lancefield T antigens. Proc. Natl. Acad. Sci. U. S. A. **102:**15641–15646. http://dx.doi.org/10.1073/pnas.0507808102.
18. **Horton RM, Cai ZL, Ho SN, Pease LR.** 1990. Gene splicing by overlap extension: tailor-made genes using the polymerase chain reaction. Biotechniques **8:**528–535.
19. **Caparon MG, Scott JR.** 1991. Genetic manipulation of pathogenic streptococci. Methods Enzymol. **204:**556–586.
20. **Framson PE, Nittayajarn A, Merry J, Youngman P, Rubens CE.** 1997. New genetic techniques for group B streptococci: high-efficiency transformation, maintenance of temperature-sensitive pWV01 plasmids, and mutagenesis with Tn*917*. Appl. Environ. Microbiol. **63:**3539–3547.
21. **Wirth R, An FY, Clewell DB.** 1986. Highly efficient protoplast transformation system for *Streptococcus faecalis* and a new *Escherichia coli-S. faecalis* shuttle vector. J. Bacteriol. **165:**831–836.
22. **Frick I-M, Mörgelin M, Björck L.** 2000. Virulent aggregates of *Streptococcus pyogenes* are generated by homophilic protein–protein interactions. Mol. Microbiol. **37:**1232–1247. http://dx.doi.org/10.1046/j.1365-2958.2000.02084.x.
23. **Okuma K, Matsuura Y, Tatsuo H, Inagaki Y, Nakamura M, Yamamoto N, Yanagi Y.** 2001. Analysis of the molecules involved in human T-cell leukaemia virus type 1 entry by a vesicular stomatitis virus pseudotype bearing its envelope glycoproteins. J. Gen. Virol. **82:**821–830.
24. **Klock HE, Lesley SA.** 2009. The polymerase incomplete primer extension (PIPE) method applied to high-throughput cloning and site-directed mutagenesis. Methods Mol. Biol. **498:**91–103. http://dx.doi.org/10.1007/978-1-59745-196-3_6.
25. **Weidlich G, Wirth R, Galli D.** 1992. Sex pheromone plasmid pAD1-encoded surface exclusion protein of *Enterococcus faecalis*. Mol. Gen. Genet. **233:**161–168. http://dx.doi.org/10.1007/BF00587575.
26. **Levin PA, Kurtser IG, Grossman AD.** 1999. Identification and characterization of a negative regulator of FtsZ ring formation in *Bacillus subtilis*. Proc. Natl. Acad. Sci. U. S. A. **96:**9642–9647. http://dx.doi.org/10.1073/pnas.96.17.9642.
27. **Timoney JF, Qin A, Muthupalani S, Artiushin S.** 2007. Vaccine potential of novel surface exposed and secreted proteins of *Streptococcus equi*. Vaccine **25:**5583–5590. http://dx.doi.org/10.1016/j.vaccine.2007.02.040.
28. **Barendt SM, Land AD, Sham L-T, Ng W-L, Tsui H-CT, Arnold RJ, Winkler ME.** 2009. Influences of capsule on cell shape and chain formation of wild-type and *pcsB* mutants of serotype 2 *Streptococcus pneumoniae*. J. Bacteriol. **191:**3024–3040. http://dx.doi.org/10.1128/JB.01505-08.
29. **Caliot E, Dramsi S, Chapot-Chartier M, Courtin P, Kulakauskas S, Péchoux C, Trieu-Cuot P, Mistou M.** 2012. Role of the group B antigen of *Streptococcus agalactiae*: a peptidoglycan-anchored polysaccharide involved in cell wall biogenesis. PLoS Pathog. **8:**e1002756. http://dx.doi.org/10.1371/journal.ppat.1002756.
30. **Pagliero E, Dideberg O, Vernet T, Di Guilm A.** 2005. The PECACE domain: a new family of enzymes with potential peptidoglycan cleavage activity in Gram-positive bacteria. BMC Genomics **6:**19. http://dx.doi.org/10.1186/1471-2164-6-19.
31. **Gara SK, Grumati P, Urciuolo A, Bonaldo P, Kobbe B, Koch M, Paulsson M, Wagener R.** 2008. Three novel collagen VI chains with high homology to the α3 chain. J. Biol. Chem. **283:**10658–10670. http://dx.doi.org/10.1074/jbc.M709540200.
32. **Engvall E, Hessle H, Klier G.** 1986. Molecular assembly, secretion, and matrix deposition of type VI collagen. J. Cell Biol. **102:**703–710. http://dx.doi.org/10.1083/jcb.102.3.703.
33. **Pontes DS, de Azevedo MSP, Chatel J-M, Langella P, Azevedo V, Miyoshi A.** 2011. *Lactococcus lactis* as a live vector: heterologous protein production and DNA delivery systems. Protein Expr. Purif. **79:**165–175. http://dx.doi.org/10.1016/j.pep.2011.06.005.
34. **Nouaille S, Ribeiro L, Miyoshi A, Pontes D, Le Loir Y, Oliveira S, Langella P, Azevedo V.** 2003. Heterologous protein production and delivery systems for *Lactococcus lactis*. Genet. Mol. Res. **2:**102–111.
35. **Holmes AR, Gilbert C, Wells JM, Jenkinson HF.** 1998. Binding properties of *Streptococcus gordonii* SspA and SspB (antigen I/II family) polypeptides expressed on the cell surface of *Lactococcus lactis* MG1363. Infect. Immun. **66:**4633–4639.
36. **Dieye Y, Usai S, Clier F, Gruss A, Piard J-C.** 2001. Design of a protein-targeting system for lactic acid bacteria. J. Bacteriol. **183:**4157–4166. http://dx.doi.org/10.1128/JB.183.14.4157-4166.2001.
37. **Esteban L, Temprana C, Arguelles M, Glikmann G, Castello A.** 2013. Antigenicity and immunogenicity of rotavirus Vp6 protein expressed on the surface of *Lactococcus lactis*. Biomed. Res. Int. **2013:**298598. http://dx.doi.org/10.1155/2013/298598.
38. **Piard JC, Hautefort I, Fischetti VA, Ehrlich SD, Fons M, Gruss A.** 1997. Cell wall anchoring of the *Streptococcus pyogenes* M6 protein in various lactic acid bacteria. J. Bacteriol. **179:**3068–3072.
39. **Ribeiro LA, Azevedo V, Le Loir Y, Oliveira SC, Dieye Y, Piard J-C, Gruss A, Langella P.** 2002. Production and targeting of the *Brucella abortus* antigen L7/L12 in *Lactococcus lactis*: a first step toward food-grade live vaccines against brucellosis. Appl. Environ. Microbiol. **68:**910–916. http://dx.doi.org/10.1128/AEM.68.2.910-916.2002.
40. **Fritzer A, Senn BM, Minh DB, Hanner M, Gelbmann D, Noiges B, Henics Ts, Schulze K, Guzman CA, Goodacre J, von Gabain A, Nagy E, Meinke AL.** 2010. Novel conserved group A streptococcal proteins identified by the antigenome technology as vaccine candidates for a non-M protein-based vaccine. Infect. Immun. **78:**4051–4067. http://dx.doi.org/10.1128/IAI.00295-10.
41. **Grandi G.** 2005. Genomics and proteomics in reverse vaccines, p 379–393. *In* Microbial proteomics. John Wiley & Sons, Inc, New York, NY.
42. **Copley SD.** 2012. Moonlighting is mainstream: paradigm adjustment required. Bioessays **34:**578–588. http://dx.doi.org/10.1002/bies.201100191.
43. **Henderson B, Martin A.** 2011. Bacterial virulence in the moonlight: multitasking bacterial moonlighting proteins are virulence determinants in infectious disease. Infect. Immun. **79:**3476–3491. http://dx.doi.org/10.1128/IAI.00179-11.
44. **Wang G, Xia Y, Cui J, Gu Z, Song Y, Zhang H, Chen W.** 2013. The roles of moonlighting proteins in bacteria. Curr. Issues Mol. Biol. **16:**15–22.
45. **Adams DW, Errington J.** 2009. Bacterial cell division: assembly, maintenance and disassembly of the Z ring. Nat. Rev. Microbiol. **7:**642–653. http://dx.doi.org/10.1038/nrmicro2198.
46. **Errington J, Daniel RA, Scheffers D-J.** 2003. Cytokinesis in bacteria. Microbiol. Mol. Biol. Rev. **67:**52–65. http://dx.doi.org/10.1128/MMBR.67.1.52-65.2003.
47. **Chung K-M, Hsu H-H, Yeh H-Y, Chang B-Y.** 2007. Mechanism of regulation of prokaryotic tubulin-like GTPase FtsZ by membrane protein EzrA. J. Biol. Chem. **282:**14891–14897. http://dx.doi.org/10.1074/jbc.M605177200.
48. **Claessen D, Emmins R, Hamoen LW, Daniel RA, Errington J, Edwards DH.** 2008. Control of the cell elongation–division cycle by shuttling of PBP1 protein in *Bacillus subtilis*. Mol. Microbiol. **68:**1029–1046. http://dx.doi.org/10.1111/j.1365-2958.2008.06210.x.

49. **Steele VR, Bottomley AL, Garcia-Lara J, Kasturiarachchi J, Foster SJ.** 2011. Multiple essential roles for EzrA in cell division of *Staphylococcus aureus*. Mol. Microbiol. **80:**542–555. http://dx.doi.org/10.1111/j.1365-2958.2011.07591.x.
50. **Karimova G, Dautin N, Ladant D.** 2005. Interaction network among *Escherichia coli* membrane proteins involved in cell division as revealed by bacterial two-hybrid analysis. J. Bacteriol. **187:**2233–2243. http://dx.doi.org/10.1128/JB.187.7.2233-2243.2005.
51. **Maggi S, Massidda O, Luzi G, Fadda D, Paolozzi L, Ghelardini P.** 2008. Division protein interaction web: identification of a phylogenetically conserved common interactome between *Streptococcus pneumoniae* and *Escherichia coli*. Microbiology **154:**3042–3052. http://dx.doi.org/10.1099/mic.0.2008/018697-0.
52. **Massidda O, Nováková L, Vollmer W.** 2013. From models to pathogens: how much have we learned about *Streptococcus pneumoniae* cell division? Environ. Microbiol. **15:**3133–3157. http://dx.doi.org/10.1111/1462-2920.12189.
53. **Pinho MG, Errington J.** 2003. Dispersed mode of *Staphylococcus aureus* cell wall synthesis in the absence of the division machinery. Mol. Microbiol. **50:**871–881. http://dx.doi.org/10.1046/j.1365-2958.2003.03719.x.
54. **Hasty DL, Ofek I, Courtney HS, Doyle RJ.** 1992. Multiple adhesins of streptococci. Infect. Immun. **60:**2147–2152.
55. **Bober M, Enochsson C, Collin M, Mörgelin M.** 2010. Collagen VI is a subepithelial adhesive target for human respiratory tract pathogens. J. Innate Immun. **2:**160–166. http://dx.doi.org/10.1159/000232587.
56. **Han M, Fan L, Qin Z, Lavingia B, Stastny P.** 2013. Alleles of keratin 1 in families and populations. Hum. Immunol. **74:**1453–1458. http://dx.doi.org/10.1016/j.humimm.2013.05.003.
57. **Hasan AAK, Zisman T, Schmaier AH.** 1998. Identification of cytokeratin 1 as a binding protein and presentation receptor for kininogens on endothelial cells. Proc. Natl. Acad. Sci. U. S. A. **95:**3615–3620. http://dx.doi.org/10.1073/pnas.95.7.3615.
58. **Cruz AA, Naclerio RM, Proud D, Togias A.** 2006. Epithelial shedding is associated with nasal reactions to cold, dry air. J. Allergy Clin. Immunol. **117:**1351–1358. http://dx.doi.org/10.1016/j.jaci.2006.01.054.
59. **de Bentzmann S, Plotkowski C, Puchelle E.** 1996. Receptors in the *Pseudomonas aeruginosa* adherence to injured and repairing airway epithelium. Am. J. Respir. Crit. Care Med. **156:**166–172.
60. **Padmalayam I, Anderson B, Kron M, Kelly T, Baumstark B.** 1997. The 75-kilodalton antigen of *Bartonella bacilliformis* is a structural homolog of the cell division protein FtsZ. J. Bacteriol. **179:**4545–4552.